Rendiconti di Matematica, Serie VII
Volume 35, Roma (2014), 159 – 188

Some models for the description of the attitude dynamics

MARTA CECCARONI – ALESSANDRA CELLETTI

Abstract: *The study of rotational dynamics is of seminal importance for the description of the motion of natural and artificial bodies. In this work with are mainly interested to the attitude of spacecraft, possibly including dissipative effects, which must be accurately accounted during mission design as they might drastically change the attitude, and lead to instability and mission failure.*

In this work we review some mechanical models of rotational dynamics and provide interesting applications of some mathematical theories. The first one is the spin-orbit problem describing the motion of a satellite rotating around an internal spin-axis and moving on a Keplerian orbit around a planet. A noticeable application of KAM theory to this model will be shortly reviewed ([6]). We will also discuss dissipative tidal effects, which might act on the system. The second model is the so-called pitch-yaw-roll problem. In particular, we consider the pitch model, in which the yaw and roll angles are constantly zero; we shall also assume that one of the moments of inertia depends on time and that the atmospheric drag acts on the system. Following [21], we provide an instructive application of Melnikov's method to establish the onset of chaos by evaluating the existence of heteroclinic intersections. The third model concerns the sloshing effect acting within a spacecraft; assuming a linear motion of the fluid in the spacecraft, this problem will be mathematically described using an equivalent mechanical model by suitably combining springs, pendulums and dampers ([33]). The last model describes the effect of a variable mass (e.g., due to fuel consumption) on the attitude of the spacecraft. Following [14], this model admits an explicit solution in the case in which the container has a cylindrical shape.

1 – Introduction

Rotational dynamics has been studied by several mathematicians since the XVIII and XIX centuries; for example, seminal results on the study of the rotation of a rigid body have been given by L. Euler, A.-L. Cauchy, C.-G. Jacobi, L. Poinsot, F. Tisserand, J.-L. Lagrange, S. Kovaleskaya. At the end of the XIX century, the Italian mathematicians G. Peano and V. Volterra gave interesting contributions in

Key Words and Phrases: *Rotational dynamics – Spin-orbit problem – Sloshing – Variable mass*
A.M.S. Classification: 37N05, 70B10, 70M20.

connection with the rotation of the Earth, precisely the motion of the poles ([31, 32]) and the variation of the latitude on the surface of our planet ([38]). Since the first satellite was launched in 1957, rotational dynamics has gained a renewed interest as far as applications to the astrodynamics of artificial satellites are concerned, thus opening a new field of research, where effects pertaining to artificial bodies are taken into account ([18, 34, 40]).

In this work we are mainly interested in the study of the attitude dynamics of artificial bodies, although some of the models we shall present apply equally well to natural bodies, where the researches on rotational dynamics have led to astonishing results. Just to quote two cases:

- the chaotic rotation of Hyperion has been the first example of chaotic dynamics in the Solar system ([41]);
- the Moon has been shown to play a relevant rôle in the stabilization of the rotation of the Earth ([23, 24]), since without our companion satellite, the Earth would be led to tumble chaotically.

Concerning artificial satellites, there exists a number of dissipative disturbances influencing both the attitude and orbital dynamics of a spacecraft which might, in some cases, deeply affect its motion causing undesired and unexpected effects. These dissipations must be carefully taken into account during the design phases of a space mission, as they might drastically change the dynamical evolution of the system, possibly introducing instability and chaos, and eventually leading even to mission failure.

The aim of this work is to provide a survey of some models describing the attitude dynamics of a spacecraft in orbit around a planet (*e.g.*, the Earth), and subject to its gravitational force. We will also consider dissipative effects caused by tides, atmospheric drag, sloshing and variable mass. It must be remarked that, although the methodologies used here to derive the various models are general, the relevance of each effect in changing the attitude of the spacecraft deeply depends on several factors like the shape and the composition of the spacecraft, or the altitude of the orbit. For this reason some conceivable assumptions on the spacecraft or on its orbit around the planet will be done.

The importance of including the disturbances due to dissipations in the mission design phase is nowadays well established. Indeed, the lack of theoretical understanding and accurate prediction of the effects of this phenomena leads to diversion or failures of space missions. Among these a noticeable example of unpredicted dissipation-induced instability in attitude dynamics is the mission failure of Explorer-I. Launched in January 1958 (shortly after the Russian Sputniks), the long and narrow shaped Explorer I was supposed to rotate around its minimum moment of inertia axis. However, after a single revolution around the Earth, it flipped over and started windmilling (*i.e.*, spinning end to end in its *maximum moment of inertia mode*). This instability was caused by a flexing of its antennae, which dis-

sipated a small amount of rotational energy thus causing the mission failure ([20]). A full range of position/velocity sensors and control torque actuators are nowadays included on each vehicle, in order to avoid such failures. These actuators counterbalance the un-modeled dissipative effects experienced by the spacecraft, adding costs to the mission and reducing the payload onboard.

Dissipative effects interact with the spacecraft's attitude as applied torques around the center of mass. They are usually categorized as internal and external (see [12] and [22]). Internal torques are self-generated torques which raise inside the spacecraft. They are, in general, the outcome of moving internal parts (thus the spacecraft cannot be considered as completely rigid). External torques are caused by environmental sources (as such they are usually referred to as environmental torques). As it is well known, the absence of external torques implies the preservation of the angular momentum about the center of mass; however, the internal torques redistribute the angular momentum in a body reference frame, altering the system's rotational energy and thus causing dissipation. Environmental torques instead directly dissipate the rotational energy of the system.

Internal torques are mainly caused by: the non perfect rigidity of the spacecraft (see the pitch model introduced in Section 3.4), the sloshing of the liquid inside partially filled tanks (see Section 4.1), the variable mass effect (see Section 4.2), the motion of internal hardware and crew. It is worth noticing that such effects depend on the sole attitude of the spacecraft and can thus be considered as independent on the orbit of the spacecraft.

On the other hand, environmental dissipative torques, depending on both the attitude and the position of the spacecraft along the orbit, comprehend: tidal effects (see Section 3.3), atmospheric drag (see Section 3.4), solar radiation pressure and magnetic torque. Actually there exists a third category of dissipative disturbances changing the attitude of a spacecraft due to the effects of the thermic excitation of the spacecraft, which, as for the environmental torques, are linked both to the position along the orbit and the attitude of the spacecraft. We will not deal with thermic effects and we also remark that the coupled (attitude/orbit) dynamics is beyond the scope of this work.

In the following sections we will focus on four main models of attitude dynamics, providing an accurate mathematical description and, when available, some applications of mathematical theories and methods. Precisely, we will review the spin-orbit problem (Section 3.3), which has applications to both natural and artificial satellites; for this model relevant stability results have been found ([6, 7]) by means of suitable applications of the celebrated Kolmogorov-Arnold-Moser (KAM) theory ([19, 1, 29]). We will also consider tidal effects due to the non-rigidity of the satellite. A model related to the spin-orbit problem is the so-called pitch-yaw-roll model (see Section 3.4) and the subcase given by the pitch model (see Section 3.4.2) that, following [21], we will extend to encompass the case of a moment of inertia depending on time; we will also include a small air drag acting on the system. For

the pitch problem the onset of chaos will be established by a nice application of Melnikov's theory ([27], see also [16]).

The last two models concern dissipative effects which arise from internal factors. In particular, we will review the sloshing effect (Section 4.1), caused for example by the motion of the fuel inside the spacecraft. In this case, it is convenient to introduce an *equivalent mechanical model*, that approximates the effect of the sloshing by using an equivalent mechanical object – pendulum, spring, etc. – whose dynamical behavior is well known. By *equivalent* it is stressed that the effects produced by such a mechanical object on the whole system are approximately the same as those provoked by the dissipative disturbance. Although being an approximation, the use of the equivalent mechanical model noticeably simplifies the mathematical problem allowing to integrate the effects of the dissipative disturbances into the equations of motion of the satellite, thus obtaining a deep mathematical insight of the dynamical evolution of the perturbed system.

The last model will concern the *variable mass* problem (Section 4.2), which occurs for example after fuel consumption. The investigation of the variable mass problem dates back to the beginning of the XIX century and it was first considered by the mathematician Graf Georg von Buquoy, when in [4] he studied the following problem (see also [35]):

"Consider an ideally flexible fibre lying reeled on a horizontal plane. Determine its motion when a constant vertical force (directed upward) is exerted on the end of the fibre".

The variable mass problem was later considered within astronomical applications by H. Gylden ([17]), while looking at the motion of comets, and by J.E. Littlewood ([26]) within a two-body problem. Precisely, Littlewood considered a unit mass moving on an ellipse under a central force of the type α/r^2, where it is assumed that α varies slowly with time with *slowness* parameter ε and tends to a limit as time goes to infinity. Littlewood's remarkable result can be summarized as follows: let $e(0)$ be the eccentricity at the initial time with $|e(0)| < b < 1$ for some $b > 0$ and let $e(t)$ be the eccentricity at time t; under suitable conditions on $\alpha = \alpha(t)$, it is found that e^2 is an adiabatic invariant, namely e^2 is constant up to terms of $O(\varepsilon)$.

We remark that in our work we are interested in studying the effect on the attitude (and not on the orbit) of the variation of the mass. The corresponding model strongly depends on the shape of the satellite and shows increasing difficulty as the form of the container looks closer to a real spacecraft. However, we will show that an elegant solution of the attitude equations of motion can be found when considering a cylinder shape (compare with [14]).

This paper is organized as follows. In Section 2 we provide the necessary tools to study the rotational dynamics, most notably Euler's angles and Euler's equations. In Section 3 we consider two models, in particular the spin-orbit problem and the pitch-yaw-roll model. In Section 4 we investigate the effects of internal dissipations, precisely the sloshing problem and a variable mass system.

2 – Prerequisites: Euler's equations

Most of the models we are going to present in the next sections make use of the classical description of the attitude dynamics in terms of the so-called Euler's angles from which Euler's equations describing the rotational motion are derived. Although this topic is discussed in many classical textbooks, for self-consistency of the present exposition we think worthwhile to give a short introduction to Euler's equations.

2.1 – Euler's angles

A rigid body with a fixed point can be moved from one orientation to another by a single rotation. We denote by (O', x, y, z) an *inertial frame* with origin O' fixed in space. Let (O, x, y, z) be a reference frame with origin coinciding with the center of mass O of the body and axes parallel to the inertial frame; we refer to this frame as the *quasi-inertial frame*, as we will allow the barycenter to move for example on an elliptic orbit as in Figure 1. Let (O, ξ, η, ζ) be a reference frame with origin in the barycenter of the body and axes coinciding with the directions of the principal axes of inertia; we refer to this frame as the *body-frame*.

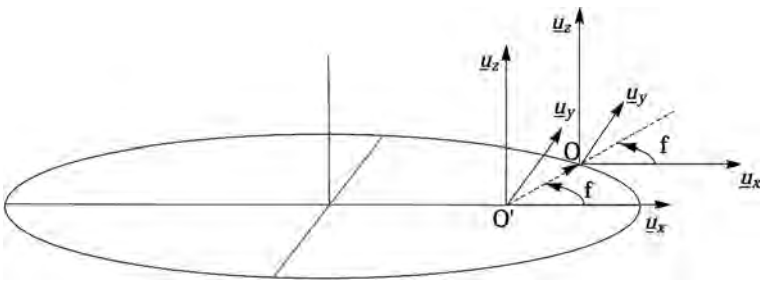

Figure 1 The inertial (O', x, y, z) and quasi-inertial (O, x, y, z) frames with unit vectors $\underline{u}_x$, $\underline{u}_y$, $\underline{u}_z$. The angle f denotes the *true anomaly*, namely the angle between the direction of $\underline{u}_x$ and that of $O'O$.

To define the orientation of a body with respect to the quasi-inertial frame we provide the rotation matrix that brings the corresponding reference axes to coincide with the body-frame.

It is well known that each element of the group of all the rotations $SO(3)$ can be expressed as the composition of three elementary rotations about three predefined axes. The orientation of the body can therefore be expressed by means of the so-called Euler angles, which we denote as φ, θ, ψ. These angles correspond to the following sequence of rotations: first about the z axis of an angle φ, the so-called *precession angle*; this rotation generates an axis N after the rotation of the x-axis. Then, we rotate around the N-axis of an angle θ, called *nutation angle*,

which generates the axis ζ provided by the rotation of the vertical axis. Finally, we perform a rotation about the ζ-axis of an angle ψ, the *proper rotation angle*.

The change of coordinates from the quasi-inertial frame to the body-frame is given by

$$\mathcal{M} = R_3(\varphi)R_1(\theta)R_3(\psi) \ ,$$

where $R_j(\gamma)$ denotes the rotation of angle γ around the j-th axis. The rotations just described are displayed in Figure 2.

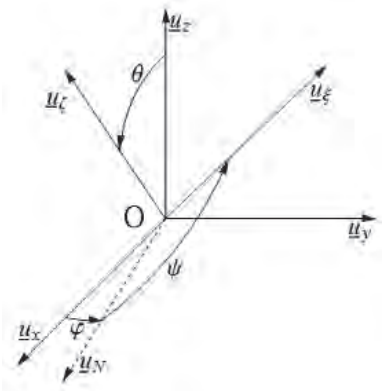

Figure 2 The body (O, ξ, η, ζ) and quasi-inertial (O, x, y, z) frames. The line of nodes N is identified by its unit vector $\underline{u}_N$. The Euler angles are denoted as (φ, θ, ψ).

2.2 – Euler's equations

The angular velocity $\underline{\omega}$ describing the orientation in time of the body can be expressed as

$$\underline{\omega} = \dot{\varphi}\underline{u}_z + \dot{\theta}\underline{u}_N + \dot{\psi}\underline{u}_\zeta \ , \tag{2.1}$$

where we have introduced the following unit vectors in the quasi-inertial frame:

$$\begin{aligned} \underline{u}_z &= (0,0,1)^T \\ \underline{u}_N &= R_3(\varphi)(1,0,0)^T = (\cos\varphi, \sin\varphi, 0)^T \\ \underline{u}_\zeta &= \mathcal{M}(0,0,1)^T = (\sin\theta\sin\varphi, -\cos\varphi\sin\theta, \cos\theta)^T \ . \end{aligned} \tag{2.2}$$

From (2.1)-(2.2) the components of $\underline{\omega} = (\omega_x, \omega_y, \omega_z)^T$ in the quasi-inertial frame are given by

$$\begin{aligned} \omega_x &= \dot{\theta}\cos\varphi + \dot{\psi}\sin\theta\sin\varphi \\ \omega_y &= -\dot{\psi}\cos\varphi\sin\theta + \dot{\theta}\sin\varphi \\ \omega_z &= \dot{\varphi} + \dot{\psi}\cos\theta \ . \end{aligned}$$

In the body-frame, instead, it results:

$$\begin{aligned} \underline{u}_z &= (\sin\theta\sin\psi, \cos\psi\sin\theta, \cos\theta)^T \\ \underline{u}_N &= (\cos\psi, -\sin\psi, 0)^T \\ \underline{u}_\zeta &= (0,0,1)^T \ , \end{aligned}$$

which yields $\underline{\omega} = (\omega_\xi, \omega_\eta, \omega_\zeta)^T$ with the components given by:

$$\begin{aligned} \omega_\xi &= \dot{\theta}\cos\psi + \dot{\varphi}\sin\theta\sin\psi \\ \omega_\eta &= \dot{\varphi}\cos\psi\sin\theta - \dot{\theta}\sin\psi \\ \omega_\zeta &= \dot{\psi} + \dot{\varphi}\cos\theta \ . \end{aligned} \tag{2.3}$$

Euler's equations are an analytic tool to study the rotational dynamics of a rigid body; they are derived from the fundamental angular momentum equation, which in the body-frame has the form:

$$\frac{d\underline{G}}{dt} + \underline{\omega} \wedge \underline{G} = \underline{M} \ ,$$

where $\underline{G}$ is the angular momentum and $\underline{M}$ is the torque generated by the external forces acting on the spacecraft. From the expression of the angular momentum ([2]) in terms of the matrix of inertia I and the angular velocity $\underline{\omega}$, say

$$\underline{G} = I\underline{\omega} \ ,$$

we obtain Euler's equations for the attitude dynamics as

$$\begin{aligned} I_{\xi\xi}\dot{\omega}_\xi + (I_{\zeta\zeta} - I_{\eta\eta})\omega_\eta\omega_\zeta &= M_\xi \\ I_{\eta\eta}\dot{\omega}_\eta + (I_{\xi\xi} - I_{\zeta\zeta})\omega_\zeta\omega_\xi &= M_\eta \\ I_{\zeta\zeta}\dot{\omega}_\zeta + (I_{\eta\eta} - I_{\xi\xi})\omega_\xi\omega_\eta &= M_\zeta \ , \end{aligned} \tag{2.4}$$

where $M = (M_\xi, M_\eta, M_\zeta)$ in the body-frame, I is the principal moment of inertia matrix with the principal axes of inertia $(I_{\xi\xi}, I_{\eta\eta}, I_{\zeta\zeta})$ on the diagonal, while $(\omega_\xi, \omega_\eta, \omega_\zeta)$ are given by (2.3). Some mechanical models which will be presented in the following sections are derived from equations (2.4).

3 – Attitude dynamics in the spin-orbit and PYR problems

In this section the attitude dynamics is analyzed using two models, which assume a non-spherical shape of the body, subject to the gravitational attraction of a host planet and possibly affected by dissipative forces. Precisely, we will discuss the models known as the *spin-orbit* (see Section 3.3) and the *pitch-yaw-roll* (hereafter PYR, see Section 3.4) problems. In both cases the orbit of the body around the planet is assumed to be Keplerian. Therefore, since the orbit is not changing with time, no attitude-orbit coupling will be considered.

3.1 – Center-pointing and fixed-direction equilibrium solutions

We consider a small body, typically an artificial satellite, moving around a planet. Having this in mind, attention must be focussed on particular families of attitude solutions suitable for spacecraft missions, in the sense that the orientation and communication requirements of an artificial satellite must be considered. In particular, we look for equilibrium solutions in which the spacecraft points a fixed direction in space or points constantly the center of the host planet (so-called *center-pointing equilibrium* solutions).

In the former case the spacecraft is pointing toward a fixed direction in the inertial frame, *e.g.* the Sun, whose distance from the spacecraft is much bigger than the semimajor axis of the orbit of the spacecraft around the attracting body, so that the Sun-spacecraft direction can be considered as fixed during the whole orbit of the satellite. In the latter case instead, a direction fixed in the satellite follows the position vector describing the motion of the spacecraft through the orbit.

In the following sections we concentrate on the *center-pointing* equilibrium solutions, by introducing two particular dynamical models of a rigid body orbiting an attracting planet, both obtained imposing that the spin-axis is always perpendicular to the orbital plane: the spin-orbit and the pitch-yaw-roll problems will be presented, respectively, in Sections 3.3 and 3.4. In particular, the solution where the spacecraft spins with the same period needed to complete an orbit around the planet is the so-called $1:1$ *resonant* solution in which a fixed direction in the spacecraft constantly points the host planet. To write the equations of motion describing such problems we need to specify equations (2.4), when the external force is given by the gravitational attraction of the planet; this task will be accomplished in Section 3.2.

3.2 – The gravitational torque

The gravitational torque results from the variation of the gravitational force over the distributed mass of the spacecraft. This torque gains relevance for large spacecraft in low altitude orbits. By Newton's law, the gravitational potential U_g acting on the spacecraft is given by

$$U_g = -\mathcal{G}M_P \int_V \frac{\rho(\underline{r})}{|\underline{R}+\underline{r}|}\, dV \ ,$$

where $\mathcal{G}$ is the gravitational constant, M_P is the mass of the attracting planet, ρ denotes the density, $\underline{R}$ the position vector of the center of mass O with respect to the inertial frame, $\underline{r}$ the position vector of the infinitesimal element of volume dV from the center of mass O of the spacecraft. Setting $r = |\underline{r}|$ and $R = |\underline{R}|$ with $r << R$, the gravitational momentum takes the form

$$\underline{M}_g = -\mathcal{G}M_P \int_V \rho(\underline{r})\ \underline{r} \wedge \frac{\underline{R}+\underline{r}}{|\underline{R}+\underline{r}|^3}\, dV \ .$$

Expanding $1/|\underline{R}+\underline{r}|^3$ in series around $r/R \simeq 0$ up to first order and taking into account that

$$\int_V \rho(\underline{r})(\underline{R}+\underline{r})dV = 0 \ ,$$

due to the definition of barycenter of the body, we obtain:

$$\underline{M}_g = 3\frac{\mathcal{G}M_P}{R^5}\int_V \rho(\underline{r})\ (\underline{r}\cdot\underline{R})\,[\underline{r}\wedge(\underline{R}+\underline{r})]\ dV \ ,$$

which is equivalent to:

$$\underline{M}_g = \frac{3\mathcal{G}M_P}{R^3}\underline{u}_R \wedge I\underline{u}_R \ ,$$

where $\underline{u}_R = \underline{R}/R$ is the unit vector of the direction of $\underline{R}$ and due to the definition of the principal moment of inertia matrix I.

Expressing the momentum in the body-frame, say $\underline{M}_g = (M_{g\xi}, M_{g\eta}, M_{g\zeta})$, we get:

$$\begin{aligned}
M_{g\xi} &= \frac{3\mathcal{G}M_P}{R^3}(I_{\zeta\zeta}-I_{\eta\eta})(\underline{u}_R\cdot\underline{u}_\eta)(\underline{u}_R\cdot\underline{u}_\zeta)\\
M_{g\eta} &= \frac{3\mathcal{G}M_P}{R^3}(I_{\xi\xi}-I_{\zeta\zeta})(\underline{u}_R\cdot\underline{u}_\zeta)(\underline{u}_R\cdot\underline{u}_\xi)\\
M_{g\zeta} &= \frac{3\mathcal{G}M_P}{R^3}(I_{\eta\eta}-I_{\xi\xi})(\underline{u}_R\cdot\underline{u}_\xi)(\underline{u}_R\cdot\underline{u}_\eta) \ .
\end{aligned} \tag{3.1}$$

Setting $(M_\xi, M_\eta, M_\zeta) = (M_{g\xi}, M_{g\eta}, M_{g\zeta})$ in (2.4) with $(M_{g\xi}, M_{g\eta}, M_{g\zeta})$ as in (3.1) and complementing these equations with (2.3), we obtain the equations describing the attitude dynamics in the body-frame of a spacecraft orbiting an attracting planet and perturbed by its gravitational torque:

$$\begin{aligned}
\dot\varphi &= \frac{1}{\sin\theta}(\omega_\eta\cos\psi+\omega_\xi\sin\psi)\\
\dot\theta &= \omega_\xi\cos\psi-\omega_\eta\sin\psi\\
\dot\psi &= \omega_\zeta-\cot\theta(\omega_\xi\sin\psi+\omega_\eta\cos\psi)\\
I_{\xi\xi}\dot\omega_\xi+(I_{\zeta\zeta}-I_{\eta\eta})\omega_\eta\omega_\zeta &= \frac{3\mathcal{G}M_P}{R^3}(I_{\zeta\zeta}-I_{\eta\eta})(\underline{u}_R\cdot\underline{u}_\eta)(\underline{u}_R\cdot\underline{u}_\zeta)\\
I_{\eta\eta}\dot\omega_\eta+(I_{\xi\xi}-I_{\zeta\zeta})\omega_\zeta\omega_\xi &= \frac{3\mathcal{G}M_P}{R^3}(I_{\xi\xi}-I_{\zeta\zeta})(\underline{u}_R\cdot\underline{u}_\zeta)(\underline{u}_R\cdot\underline{u}_\xi)\\
I_{\zeta\zeta}\dot\omega_\zeta+(I_{\eta\eta}-I_{\xi\xi})\omega_\xi\omega_\eta &= \frac{3\mathcal{G}M_P}{R^3}(I_{\eta\eta}-I_{\xi\xi})(\underline{u}_R\cdot\underline{u}_\xi)(\underline{u}_R\cdot\underline{u}_\eta) \ .
\end{aligned} \tag{3.2}$$

We remark that, if we assume that the spacecraft orbits around a planet located in the origin O' of the inertial frame, then, denoting by f the true anomaly, we have

$$\underline{R} = R\ (\cos f, \sin f, 0)$$

with

$$R \equiv |\underline{R}| = \frac{a(1-e^2)}{1+e\cos f} \ ,$$

where a and e are the semimajor axis and the eccentricity of the Keplerian orbit. In the following, we shall always take normalized units of measure, so that $\mathcal{G} = 1$, $M_P = 1$, $a = 1$.

3.3 – The spin-orbit model

The equations in (3.2) describe the attitude dynamics of a spacecraft under the gravitational influence of an attracting body. In this section we derive the equations of motion governing the spin-orbit model ([6, 8]), which are obtained under the following hypotheses. We consider a triaxial satellite with an ellipsoidal shape, orbiting on a Keplerian ellipse around a planet. We assume that:

(*i*) the spin axis is perpendicular to the orbit plane;
(*ii*) the spin axis coincides with the shortest physical axis (namely, the axis with largest moment of inertia), *i.e.* $\underline{u}_\zeta = \underline{u}_z$ with $I_{\zeta\zeta} > I_{\eta\eta} > I_{\xi\xi}$;
(*iii*) the dissipative effects as well as all the perturbations due to other planets or satellites are neglected.

We denote by $T_{\rm orb}$ and $T_{\rm rot}$, respectively, the orbital period of the satellite around the planet and the rotational period of the satellite around its spin-axis.

Definition 3.1. A spin-orbit resonance of order $p : q$ for $p, q \in \mathbb{Z}$ with $q \neq 0$ occurs whenever the ratio of the orbital and rotational periods is equal to p/q:

$$\frac{T_{\rm orb}}{T_{\rm rot}} = \frac{p}{q} \ .$$

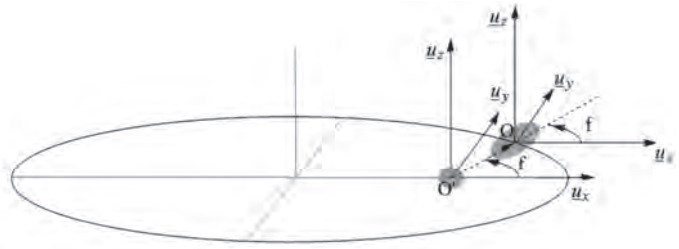

Figure 3 The spin-orbit model in the inertial (O', x, y, z) and quasi-inertial (O, x, y, z) frames with unit vectors $\underline{u}_x$, $\underline{u}_y$, $\underline{u}_z$. The angle f denotes the true anomaly.

As far as natural bodies are concerned, remarkable resonances are the 1:1 and 3:2 resonances. The Moon as well as most of the largest satellites of the giant planets

are found in a 1:1 spin-orbit resonance; this dynamical configuration implies that the satellite always points the same face to the host planet. Mercury is an example of a 3:2 spin-orbit resonance with the Sun, which implies that during 2 revolutions around the Sun, Mercury makes 3 rotations about its spin-axis ([10, 13, 25]).

The spin-orbit model is mainly used to describe the motion of planets and natural satellites, for which resonant and non-resonant solutions are of interest. However, for the study of the attitude dynamics of an artificial satellite, the $1:1$ resonance can be conveniently investigated, since it corresponds to a spacecraft constantly pointing the orbited planet.

In order to derive the equations of motion describing the spin-orbit model, we start by remarking that by the assumptions (i)-(iii) above, one can impose that $\underline{u}_\zeta \equiv \underline{u}_z$. Special care must be taken with this setting, since it is equivalent to let θ be constantly equal to zero in (3.2), which corresponds to a singularity of the Euler's angles representation. However, it is easy to see that by setting $\theta = 0$, the transformation from the quasi-inertial frame to the body-frame is obtained by making a single rotation around the ζ axis of angle ψ. In this case $\mathcal{M} = R_3(\psi)$ and thus we obtain $\underline{\omega} = (\omega_\xi, \omega_\eta, \omega_\zeta)^T = (0, 0, \dot{\psi})^T$.

In the quasi-inertial frame we can write $\underline{u}_R = \cos f \underline{u}_x + \sin f \underline{u}_y$, while in the body-frame it is:

$$\underline{u}_R = \mathcal{M}^T \begin{pmatrix} \cos f \\ \sin f \\ 0 \end{pmatrix} = \begin{pmatrix} \cos f \cos\psi + \sin f \sin\psi \\ \sin f \cos\psi - \cos f \sin\psi \\ 0 \end{pmatrix} = \begin{pmatrix} \cos(f-\psi) \\ \sin(f-\psi) \\ 0 \end{pmatrix} .$$

Thus, we obtain that (3.2) reduces to

$$\begin{aligned} \dot{\psi} &= \omega_\zeta \\ \dot{\omega}_\zeta &= \frac{3}{2}\left(\frac{1+e\cos f}{1-e^2}\right)^3 \frac{I_{\eta\eta} - I_{\xi\xi}}{I_{\zeta\zeta}} \sin\left(2(f-\psi)\right) , \end{aligned}$$

which is equivalent to

$$\ddot{\psi} + \frac{3}{2}\left(\frac{1+e\cos f}{1-e^2}\right)^3 \frac{I_{\eta\eta} - I_{\xi\xi}}{I_{\zeta\zeta}} \sin(2\psi - 2f) = 0 . \tag{3.3}$$

We introduce the quantity $\varepsilon \geq 0$ defined as

$$\varepsilon = \frac{3}{2}\frac{I_{\eta\eta} - I_{\xi\xi}}{I_{\zeta\zeta}} , \tag{3.4}$$

which is proportional to the equatorial oblateness of the satellite. We notice that in case of equatorial symmetry, then $\varepsilon = 0$ and equation (3.3) is trivially integrable. We also remark that the true anomaly f depends on the eccentricity; in particular, for $e = 0$ the true anomaly reduces to the time and (3.3) is again integrable (see [8]). We report in Figure 4 the Poincaré sections associated to (3.3) around the 1:1 resonance for different values of the eccentricity and the parameter in (3.4).

3.3.1 – Stability of rotational and librational tori

The Poincaré maps of the spin-orbit problem presented in Figure 4 show a structure very close to that of a pendulum, where a periodic orbit (*e.g.*, the synchronous resonance) is surrounded by librational tori, while the chaotic separatrix through the unstable equilibria divides the librational zone from the region in which rotational tori can be found. A rigorous proof of the existence of rotational and librational tori can be obtained by KAM theory ([6, 7, 8]). To this end, we start by remarking that equation (3.3) is associated to the following one-dimensional, time-dependent Hamiltonian function:

$$H(\Psi, \psi, t) = \frac{1}{2}\Psi^2 - \frac{1}{2}\varepsilon \left(\frac{a}{R(t)}\right)^3 \cos(2\psi - 2f(t)) \ , \tag{3.5}$$

where ε is as in (3.4) and Ψ is the action conjugated to ψ. For the Hamiltonian (3.5) we have the important remark that the two-dimensional rotational KAM tori separate the three-dimensional phase space into invariant regions, thus giving a strong stability property in the sense of confinement of the motion within invariant surfaces.

As it is well known, KAM theory provides a constructive algorithm to compute concrete estimates on the perturbing parameter (*i.e.*, the parameter ε in (3.5)), which guarantee the persistence of an invariant torus with preassigned frequency. The theorem can be applied provided the Hamiltonian is non-degenerate, namely the Hessian of the unperturbed part is different from zero (which is the case for (3.5)), and the frequency ω_t of the torus satisfies a strong non-resonance condition, namely a Diophantine inequality of the form

$$\left|\omega_t - \frac{p}{q}\right|^{-1} \leq C|q|^2 \qquad \text{for all} \ \ p, q \in \mathbb{Z} \ , \quad q \neq 0 \ .$$

Under such conditions, KAM theory ensures the persistence of an invariant torus with frequency ω_t for any $\varepsilon \leq \varepsilon(\omega_t)$, where the threshold $\varepsilon(\omega_t)$ can be computed explicitly. To get good results, dedicated estimates as well as a computer-assisted implementation are necessary. This task has been performed in [6], where the stability of the synchronous resonance for some natural satellites has been investigated. For these bodies, the results have shown to be valid for realistic values of the parameters, namely for the true eccentricity and the true oblateness parameter ε of the celestial bodies; of course, similar estimates can be performed for artificial satellites to get an analytical proof of the stability of their rotational motions.

As far as the librational tori surrounding the periodic orbits in Figure 4 are concerned, one can still use KAM theory to prove their existence and stability, provided some preliminary steps are performed. Following [7] which considered librational tori around the 1:1 resonance, one needs to center the Hamiltonian on the periodic

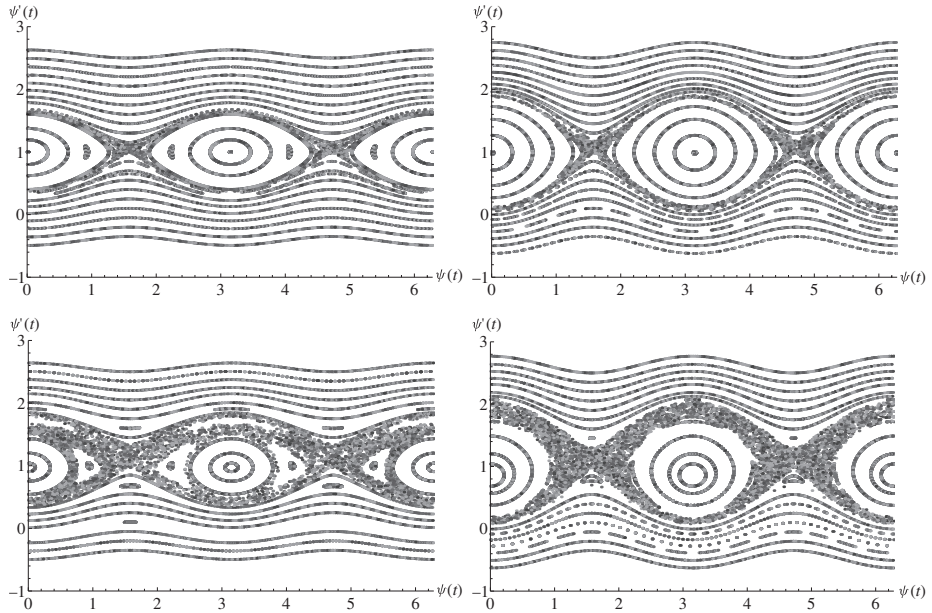

Figure 4 The 1 : 1 spin-orbit resonance for $e = 0.002$ and $\varepsilon = 0.2$, $\varepsilon = 0.4$ (upper panels, left and right respectively), $e = 0.02$ and $\varepsilon = 0.2$, $\varepsilon = 0.4$ (lower panels, left and right respectively).

orbit, to expand in Taylor series around the new origin, then to diagonalize the quadratic terms in order to obtain a harmonic oscillator, which will be perturbed by higher degree terms depending on time. Afterwards, it is convenient to introduce the action-angle variables associated to the harmonic oscillator, which allow one to implement in a simple way a Birkhoff normalization, which aims to reduce the size of the perturbation. The final step will be the implementation of KAM theory to prove the existence of the librational torus. This procedure has been successfully performed in [7], where the existence of librational tori surrounding the synchronous resonance has been proven for some natural satellites with estimates on the parameters in full agreement with the astronomical expectations.

3.3.2 – Tidal effect

Among the dissipative effects we have neglected in writing equation (3.3) describing the spin-orbit problem, a relevant rôle is played by the tidal effect induced by the non-rigidity of the satellite. The corresponding tidal torque can be written as a function having a linear dependence on the angular velocity (see, *e.g.*, [15], [30]):

$$\mathcal{T}(\dot{\psi}, t; e) = -C_d \left[\mathcal{L}(t; e)\dot{\psi} - \mathcal{N}(t; e) \right] ,$$

where the functions $\mathcal{L}, \mathcal{N}$ are defined as (recall that f depends on time)

$$\mathcal{L}(t;e) = \left(\frac{1+e\cos f}{1-e^2}\right)^6 , \qquad \mathcal{N}(t;e) = \left(\frac{1+e\cos f}{1-e^2}\right)^6 \dot{f} .$$

The dissipative factor C_d depends on the physical and orbital properties of the satellite (mass, density, internal structure, etc.).

Taking the averages $\bar{\mathcal{L}}, \bar{\mathcal{N}}$ of $\mathcal{L}, \mathcal{N}$ (compare with [11]), one obtains the expressions:

$$\begin{aligned} \bar{\mathcal{L}}(e) &\equiv \frac{1}{(1-e^2)^{9/2}} \left(1 + 3e^2 + \frac{3}{8}e^4\right) , \\ \bar{\mathcal{N}}(e) &\equiv \frac{1}{(1-e^2)^6} \left(1 + \frac{15}{2}e^2 + \frac{45}{8}e^4 + \frac{5}{16}e^6\right) . \end{aligned} \tag{3.6}$$

In conclusion, the equation of motion of the spin-orbit problem with an averaged dissipative tidal effect is given by

$$\ddot{\psi} \; + \varepsilon \left(\frac{1+e\cos f}{1-e^2}\right)^3 \sin(2\psi - 2f) = -C_d\Big[\bar{\mathcal{L}}(e)\dot{\psi} - \bar{\mathcal{N}}(e)\Big] \tag{3.7}$$

with $\bar{\mathcal{L}}, \bar{\mathcal{N}}$ as in (3.6). We remark that the persistence of KAM invariant attractors for systems like (3.7) has been treated in [5, 9] to which we refer for full details.

3.4 – Pitch-Yaw-Roll model

The pitch-yaw-roll (denoted with the acronym PYR) model describes the motion of an artificial satellite pointing the attracting planet around which it orbits ([21]), although along a direction different from that in which the spin-orbit problem points the planet and using a different set of angles. In particular, such model is obtained by (3.2) with some further hypotheses; it shares with the spin-orbit model the assumption that the spin axis $\underline{u}_\omega = \underline{\omega}/|\underline{\omega}|$ is perpendicular to the orbital plane. However, in contrast with the spin-orbit model, in the PYR problem the axis η of the body-frame is perpendicular to the orbital plane, pointing opposite with respect to the angular velocity vector of the spacecraft along the orbit.

3.4.1 – PYR equations of motion

In order to investigate the dynamics of the PYR model, we need to introduce a reference frame to which we refer as the *PYR-frame* (O, X, Y, Z) with center O and with the axes defined as follows. The $\underline{u}_Z$ unit vector constantly points the center of mass O' of the planet, the $\underline{u}_X$ unit vector of the X axis is contained in the orbit plane, it is perpendicular to $\underline{u}_Z$ and points the same direction of the velocity vector

of the spacecraft along the orbit (notice that it is not, in general, parallel to the velocity due to the non-zero eccentricity of the orbit). Finally, the unit vector $\underline{u}_Y$ is set normal to the orbit plane, completing a positively oriented reference frame. Using standard terminology in Astrodynamics, the X, Y, Z axes are called *roll*, *pitch*, *yaw* axes.

The attitude of the body is provided by the rotation that brings the PYR-frame to coincide with the body-frame. This rotation is obtained through three elementary rotations, but, this time, the first one about $\underline{u}_Z$ of an angle Ψ (yaw), the second *clockwise* of an angle Θ (pitch) about $\underline{u}_{Y'}$ with $\underline{u}_{Y'} = R_3(\Psi)\underline{u}_Y$. Finally, we perform a third rotation of an angle Φ (roll) about $\underline{u}_\xi = R_3(\Psi)R_2(\Theta)\underline{u}_X$.

The collection of the three angles Φ, Θ, Ψ is sometimes considered as a particular set of Euler angles, also known as Cardan or Tait-Bryan angles.

The change of coordinates relating the PYR and body frames is given by

$$\begin{pmatrix} X \\ Y \\ Z \end{pmatrix} = \mathcal{N}^T \begin{pmatrix} \xi \\ \eta \\ \zeta \end{pmatrix} ,$$

where $\mathcal{N}^T = R_3(\Psi)R_2(\Theta)R_1(\Phi)$. Furthermore, the change from the quasi-inertial frame to the PYR-frame (see Figure 5) is given by the following matrix $\mathcal{W}$:

$$\mathcal{W} = R_1\left(-\frac{3}{2}\pi\right) R_3\left(-\left(\frac{\pi}{2} + f\right)\right) ,$$

such that

$$\begin{pmatrix} X \\ Y \\ Z \end{pmatrix} = \mathcal{W} \begin{pmatrix} x \\ y \\ z \end{pmatrix} .$$

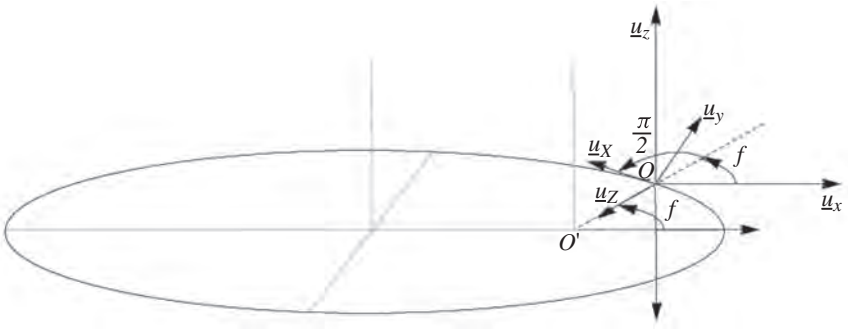

Figure 5 The PYR (O, X, Y, Z) and quasi-inertial (O, x, y, z) frames, where O revolves on a Keplerian ellipse around O'; f denotes the true anomaly.

As a consequence, we obtain that $\mathcal{M}^T\mathcal{W}^T = \mathcal{N}$, which provides the relation between the roll, pitch, yaw angles and the Euler angles as well as the true anomaly f, namely:

$$\varphi = f - \arctan\left(-\frac{\cos\Theta\cos\Phi}{-\cos\Phi\cos\Psi\sin\Theta + \sin\Phi\sin\Psi}\right)$$
$$\psi = \arctan\left(\frac{\cos\Theta\sin\Psi}{\cos\Phi\cos\Psi - \sin\Theta\sin\Phi\sin\Psi}\right)$$
$$\theta = \arccos\left(\cos\Psi\sin\Phi + \cos\Phi\sin\Theta\sin\Psi\right) .$$

The angular velocity vector $\underline{\omega}$ of the spacecraft can be expressed in terms of the roll, pitch and yaw angles as $\underline{\omega} = \dot{\Psi}\underline{u}_Z + \dot{\Theta}\underline{u}_{Y'} + \dot{\Phi}\underline{u}_\xi$. The components of $\underline{\omega}$ in the body-frame are given by

$$\omega_\xi = \dot{\Phi} - \dot{\Psi}\sin\Theta$$
$$\omega_\eta = \dot{\Theta}\cos\Phi + \dot{\Psi}\cos\Theta\sin\Phi$$
$$\omega_\zeta = -\dot{\Theta}\sin\Phi + \dot{\Psi}\cos\Theta\cos\Phi .$$

Moreover, in the PYR-frame the vector $\underline{R}$ is always directed along the negative $\underline{u}_Z$ direction, namely $\underline{R} = -R\underline{u}_Z$. Thus, its expression in the body-frame in terms of the roll, pitch, yaw angles is given by $\underline{R} = (R\sin\Theta, -R\sin\Phi\cos\Theta, -R\cos\Phi\cos\Theta)^T$.

In conclusion, the system of equations (3.2) as a function of the roll, pitch, yaw angles takes the form:

$$\begin{aligned}
\omega_\xi &= \dot{\Phi} - \dot{\Psi}\sin\Theta \\
\omega_\eta &= \dot{\Theta}\cos\Phi + \dot{\Psi}\cos\Theta\sin\Phi \\
\omega_\zeta &= -\dot{\Theta}\sin\Phi + \dot{\Psi}\cos\Theta\cos\Phi
\end{aligned}$$

$$I_{\xi\xi}\dot{\omega}_\xi + (I_{\zeta\zeta} - I_{\eta\eta})\omega_\eta\omega_\zeta = 3\left(\frac{1+e\cos f}{1-e^2}\right)^3 (I_{\zeta\zeta} - I_{\eta\eta})\,(-\sin\Phi\cos\Theta)(-\cos\Phi\cos\Theta)$$

$$I_{\eta\eta}\dot{\omega}_\eta + (I_{\xi\xi} - I_{\zeta\zeta})\omega_\zeta\omega_\xi = 3\left(\frac{1+e\cos f}{1-e^2}\right)^3 (I_{\xi\xi} - I_{\zeta\zeta})\,(-\cos\Phi\cos\Theta)(\sin\Theta)$$

$$I_{\zeta\zeta}\dot{\omega}_\zeta + (I_{\eta\eta} - I_{\xi\xi})\omega_\xi\omega_\eta = 3\left(\frac{1+e\cos f}{1-e^2}\right)^3 (I_{\eta\eta} - I_{\xi\xi})\,(\sin\Theta)(-\sin\Phi\cos\Theta) . \quad (3.8)$$

3.4.2 – The pitch model

Setting the roll and yaw motion to be identically zero, that is $\Psi(t) = 0$ and $\Phi(t) = 0$ at any time, and assuming that the orbit of the satellite is circular, equations (3.8) become:

$$\begin{aligned}
\omega_\xi &= 0 \\
\omega_\eta &= \dot{\Theta} \\
\omega_\zeta &= 0 \\
\dot{\omega}_\xi &= 0 \\
\dot{\omega}_\eta &= -\frac{3}{2}\frac{(I_{\xi\xi} - I_{\zeta\zeta})}{I_{\eta\eta}} \sin 2\Theta \\
\dot{\omega}_\zeta &= 0 \ .
\end{aligned}$$

This system of equations is equivalent to

$$\ddot{\Theta} + \frac{3}{2}\frac{(I_{\xi\xi} - I_{\zeta\zeta})}{I_{\eta\eta}} \sin 2\Theta = 0 \ , \tag{3.9}$$

to which we refer as the equation of motion of the *pitch model*. Some Poincaré maps associated to (3.9) are shown in Figure 6.

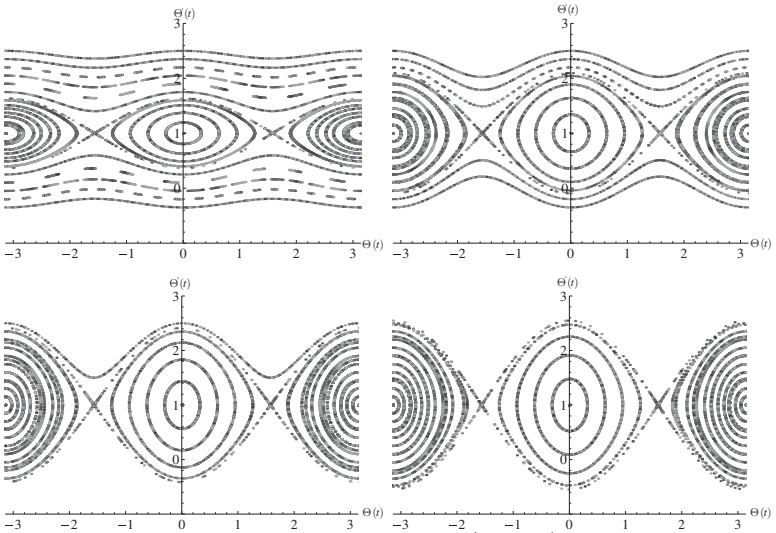

Figure 6 Poincaré maps of the pitch model (3.9) for $\frac{3}{2}\frac{(I_{\zeta\zeta}-I_{\xi\xi})}{I_{\eta\eta}} = 0.2, 0.6$ (upper panels, left and right respectively) and $\frac{3}{2}\frac{(I_{\zeta\zeta}-I_{\xi\xi})}{I_{\eta\eta}} = 1, 1.2$ (lower panels, left and right respectively).

3.4.3 – Pitch motion of a non-rigid spacecraft with viscous drag: the Melnikov's criterion

When studying the motion of a spacecraft, one is immediately led to release some assumptions which were taken in the derivation of the equation of motion (3.9) of the pitch model, precisely the fact that the spacecraft cannot be perfectly rigid and the fact that, beside the gravity gradient torque, the effect of the Earth's atmosphere must be taken into account to describe the attitude of the satellite. Along these directions, a simple model has been devised in [21], where an interesting application of Melnikov's method ([27]) is presented to show the onset of chaos for given values of the parameters. In the rest of this section we present such results, referring to [21] for full details.

We consider an asymmetric spacecraft with moments of inertia $I_{\xi\xi} > I_{\eta\eta} > I_{\zeta\zeta}$, such that $I_{\xi\xi}$ depends periodically on time as

$$I_{\xi\xi}(t) = I^0_{\xi\xi} + I^1_{\xi\xi} \cos \nu t \ , \tag{3.10}$$

where $I^0_{\xi\xi}$, $I^1_{\xi\xi}$, ν are real constants. We assume that the spacecraft is non-perfectly rigid, namely that $I^1_{\xi\xi} << I^0_{\xi\xi}$, and that the barycenter of the body is not altered by the time-dependence of the moment of inertia. We also assume that the atmosphere of the Earth acts on the satellite through a viscous drag with coefficient γ sufficiently small. Taking into account (3.9) and (3.10), we write the equation of motion describing the model of a non-rigid spacecraft with viscous drag orbiting on a circular trajectory as

$$\ddot{\Theta} = -\frac{K}{2} \sin(2\Theta) - \frac{\varepsilon}{2} \sin(2\Theta) \cos(\nu t) - \gamma \dot{\Theta} \ , \tag{3.11}$$

where $K \equiv 3\frac{I^0_{\xi\xi} - I_{\zeta\zeta}}{I_{\eta\eta}}$, $\varepsilon \equiv 3\frac{I^1_{\xi\xi}}{I_{\eta\eta}}$.

Taking into account that ε and γ are small, we start by considering the unperturbed case $\varepsilon = \gamma = 0$. In this case we obtain a one-dimensional pendulum equation

$$\ddot{\Theta} + \frac{K}{2} \sin(2\Theta) = 0 \ ,$$

which corresponds to the integrable Hamiltonian function

$$H(p_\Theta, \Theta) = \frac{1}{2} p^2_\Theta - \frac{K}{4} \cos(2\Theta) \ ,$$

where p_Θ is the momentum conjugated to Θ. It is easy to see that stable equilibria occur at $(\Theta, p_\Theta) = (\pi, 0)$ modulus π, while unstable equilibria are located at $(\Theta, p_\Theta) = (\frac{\pi}{2}, 0)$ modulus π. Let us denote by U_1 and U_2 the unstable equilibria

at $(\frac{\pi}{2}, 0)$ and $(\frac{3}{2}\pi, 0)$, respectively; these points are connected by the following four heteroclinic trajectories:

$$(\Theta^{\pm}(t), p_{\Theta}^{\pm}(t)) = \Big(\pm \arcsin(\tanh(\sqrt{K}t)),\ \pm\sqrt{K}\,\mathrm{sech}(\sqrt{K}t)\Big) \tag{3.12}$$

with the initial conditions $(\Theta^{\pm}(0), p_{\Theta}^{\pm}(0)) = (0, \pm\sqrt{K})$. Moreover, we know that the unstable manifold of U_1 coincides with the stable manifold of U_2, and that the stable manifold of U_1 coincides with the unstable manifold of U_2.

When ε and γ are not zero, the stable and unstable manifolds of U_1 and U_2 do not coincide under the perturbed dynamics and they might intersect transversally, generating an infinite sequence of heteroclinic points, so that a stochastic layer appears in the neighborhood of the unperturbed separatrices. Melnikov's method ([27, 16]) provides a criterion to evaluate the existence of such heteroclinic intersections by showing that the so-called Melnikov's function, which measures the distance between the stable and unstable manifolds of the hyperbolic points, has zeros. Referring to [27, 16] for the definition of Melnikov's function $\mathcal{M}^{\pm} = \mathcal{M}^{\pm}(t)$, borrowing the result from [21] we quote the expression for $\mathcal{M}^{\pm}$, which is obtained starting from (3.11):

$$\mathcal{M}^{\pm}(t_0) = -\int_{-\infty}^{\infty} p_{\Theta}^{\pm}(t)\ \left(\frac{\varepsilon}{2}\sin 2\Theta^{\pm}(t)\ \cos(\nu(t+t_0)) + \gamma p_{\Theta}^{\pm}(t)\right)\ dt\ , \tag{3.13}$$

where $(\Theta^{\pm}(t), p_{\Theta}^{\pm}(t))$ are the solutions (3.12) associated to the unperturbed case. Replacing (3.12) in (3.13), we obtain that the positive branch of $\mathcal{M}(t_0)$ is given by

$$\begin{aligned} \mathcal{M}(t_0) = &-\varepsilon\sqrt{K}\int_{-\infty}^{\infty} \mathrm{sech}^2(\sqrt{K}t)\ \tanh(\sqrt{K}t)\ \cos(\nu(t+t_0))\ dt \\ &-\gamma\ K\ \int_{-\infty}^{\infty} \mathrm{sech}^2(\sqrt{K}t)\ dt\ . \end{aligned} \tag{3.14}$$

A direct computation or applying the residue's method for the integrals in (3.14) gives the following expression ([21]):

$$\mathcal{M}(t_0) = \varepsilon\frac{\pi}{2}\ \frac{\nu^2}{K}\ \mathrm{cosech}\left(\frac{\pi}{2}\frac{\nu}{\sqrt{K}}\right)\ \sin(\nu t_0) - 2\gamma\sqrt{K}\ .$$

Melnikov's criterion relies on the determination of simple zeros of $\mathcal{M}(t_0)$, which occur for

$$\gamma < \gamma_c = \varepsilon\frac{\pi}{4}\ \frac{\nu^2}{K^{\frac{3}{2}}}\ \mathrm{cosech}\left(\frac{\pi}{2}\frac{\nu}{\sqrt{K}}\right)\ .$$

In conclusion, under perturbation we have the onset of chaos for $\gamma < \gamma_c$ through heteroclinic intersections between the stable and unstable manifolds of the hyperbolic equilibria of the pitch model.

4 – Attitude dynamics with internal dissipations

The dissipations acting on an artificial satellite can be divided in two main groups: the internal and the environmental dissipations. The main internal dissipative effects experienced by a spacecraft are:

- dissipation due to flexibility of the spacecraft,
- sloshing,
- variable mass torques,
- crew's motion.

As for environmental dissipations, one can have:

- magnetic torques,
- atmospheric drag.

In this section we concentrate on two internal dissipations: sloshing and variable mass. For these effects, we provide the model describing the attitude dynamics. For the sloshing problem we introduce an equivalent model based on springs, dampers and pendulums in the assumption of linear motion of the liquid. For the variable mass problem, we shall approach in Section 4.2 the model of a cylindric shaped satellite; following [14], an explicit solution will be found under some simplifying assumptions.

4.1 – Sloshing

By *sloshing* it is meant any motion of the free liquid surface inside its container. Quoting [33]: "Our everyday experience in carrying a cup of coffee or a bowl of soup may be frustrating unless we are very careful as to how we move, but may still deceive us into believing that the sloshing of the liquid is simple".

Sloshing models the free-surface oscillations of a fluid in a partially filled tank. These oscillations originate from angular oscillations around a center or linear (lateral or longitudinal) displacements. Due to disturbance type and container shape, the liquid surface can slosh in different ways, such as simple planar, nonplanar, rotational, irregular beating, symmetric, asymmetric, quasi-periodic and even chaotic motions.

The basic problem of liquid sloshing involves the estimation of hydrodynamic pressure distribution, forces, moments and natural frequencies of the free-liquid surface. These parameters affect the dynamics, stability and performance of the tanks. The dynamics loads from the fuel have inertial and dissipative components, affecting both the attitude stability of the spacecraft and the integrity of the tank structure.

The liquid sloshing problem can be faced with two different approaches: using fluid mechanics or adopting an equivalent mechanical model. Fluid mechanics,

mainly based on the so called Navier-Stokes equations, can be mathematically complex and closed-form solutions are available only for very simple cases. Alternatively, in the equivalent mechanical model approach the sloshing effect is approximated by a suitable combination of mechanical objects, such as springs, dampers, or pendulums. We shall follow this approach as a tradeoff for studying only an approximation of the real dynamics.

As we will show in the next section, an equivalent mechanical model provides a realistic representation of the dynamics of the liquid inside the tank, where the equivalence is taken in the sense of equal resulting forces and moments acting on the tank wall ([33]).

4.1.1 – Possible sloshing modes

Roughly speaking, the remaining fuel in the rigid tanks can be divided in two distinct components, one moving in unison with the tank, hereafter referred to as the solidified fuel, and one experiencing sloshing on the free surface. There are three major types of possible motion for the liquid inside the tank (see Figure 7):

- the linear planar liquid motion: which occurs in case of small oscillations, and in which the fluid surface remains planar with no rotations of its nodal diameter;
- the weakly nonlinear sloshing phenomena with large-amplitude oscillations and non-planar motions of the liquid surface;
- the strongly nonlinear fuel motion with quick fuel-velocity changes, provoked by collisions of the fuel on the tank walls.

The main equivalent mechanical models used for describing the linear motion type consists of a series of springs, dashpots and simple pendulums. We mention that for the weakly nonlinear sloshing a spherical pendulum describing relatively large oscillations may be used. Finally, for the latter case, a spherical pendulum is adopted as for the previous one, but the possibility for the pendulum to impact the walls of the tank is accounted.

In this work only the linear motion for the liquid will be taken into account; in particular, we shall derive the disturbance torque using a mass-spring-damper model.

4.1.2 – Mass-Spring-Damper Model

In order to describe properly the effects of the propellant sloshing inside the tank, some preliminary assumptions are firstly needed:

- small displacements, velocities and slope of the liquid-free surfaces;
- a rigid tank;
- non-viscous liquid;
- incompressible and homogeneous fluid.

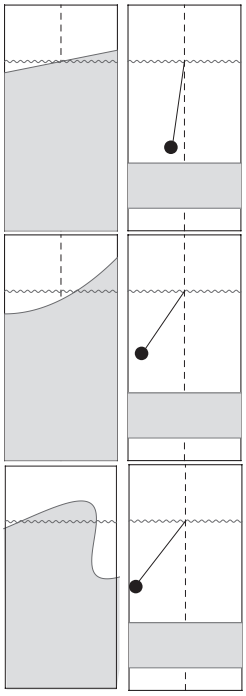

Figure 7 The three possible sloshing modes and the corresponding equivalent models ([33]): the linear planar motion (top panels), the weakly nonlinear sloshing (middle panels) and the strongly nonlinear motion (bottom panels).

Under the above assumptions the derivation provided in [33] of the so called mass-spring-damper equivalent mechanical model will be hereby described.

Let m_0 be the mass of the fuel moving unison with the tank and let m_i, $i = 1, \ldots, N$, be a series of masses, representing the equivalent mass of each sloshing mode. Each of the modal masses is restrained by a spring of elastic constant k_i and a dashpot with damping constant C_i. A dashpot is a damper, which resists the motion via viscous friction with a resulting force opposite and proportional to the velocity. Remark that both the elastic and damping constants depend on the peculiarities of the spacecraft (*e.g.*, its shape and dimensions) to which the sloshing disturbance is applied. Thus, they have to be given as data once the spacecraft is fixed.

Let m_F be the total mass of the fluid; then, the following relation must hold:

$$m_F = m_0 + \sum_{i=1}^{N} m_i \ .$$

The spacecraft will be assumed to be in rotational (oscillatory) motion around the ζ axis, passing through its center of gravity with angular velocity $-\dot{\Psi}$ and in linear

(oscillatory) motion in the $\underline{u}_\xi$ direction with linear velocity $\dot{\xi}\underline{u}_\xi$ with respect to an inertial reference frame with the axes as in Figure 8.

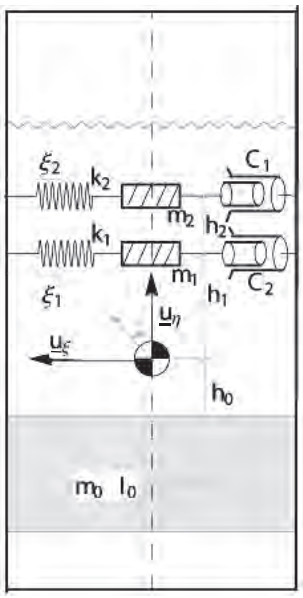

Figure 8 A sketched diagram of the mass-spring-damper model ([33]).

A schematic diagram of the equivalent mechanical model hereby introduced is shown in Figure 8. This model consists of a rigid mass m_0 (with moment of inertia I_0), moving in unison with the tank, and a series of masses m_i with $i = 1, \ldots, N$, representing the equivalent mass of each sloshing mode. Set the center of mass of the solidified fuel to be at a distance h_0 from the center of gravity along the direction $-\underline{u}_\eta$ and the modal masses at $h_i\underline{\eta}$, respectively. Moreover, each modal mass m_i is restrained by a spring k_i and a dashpot C_i. The total moment of inertia of the tank in the $\underline{u}_\eta$ direction, which passes through the center of mass of the solidified liquid, is given by

$$I_F = I_0 + m_0 h_0^2 + \sum_{i=1}^{N} m_i h_i^2 \ .$$

Since the center of mass in the $\underline{u}_\eta$ direction must be preserved, we set:

$$m_0 h_0 - \sum_{i=1}^{N} m_i h_i = 0 \ .$$

Let ξ_i be the horizontal displacements of the masses m_i relative to the tank wall (in the negative $\underline{u}_\xi$ direction), ξ be the displacement of the tank and define $-\Psi$ as

the rotational (pitch) angle about $\underline{u}_\zeta$ of the tank. The equations of motion can be derived using Lagrange's equations

$$\frac{d}{dt}\left(\frac{\partial \mathcal{L}}{\partial \dot{q}_i}\right) - \frac{\partial \mathcal{L}}{\partial q_i} = -\frac{\partial \mathfrak{I}}{\partial \dot{q}_i} + Q_i$$

with q_i the generalized coordinates, $\dot{q}_i$ the corresponding velocities, Q_i the generalized forces and $\mathfrak{I}$ the Rayleigh dissipation energy function accounting for the N dashpots. For this model, in particular, the generalized coordinates vector will be set to be $\underline{q} = (\xi, \xi_1, \ldots, \xi_N, \Psi)^T$ and thus the generalized forces will be $\underline{Q} = (-F_\xi, 0, M_\eta)^T$ (see [36]).

The kinetic and potential energies of the various components of the system are thus needed to evaluate the overall Lagrangian. Let $\underline{\omega} = (0, 0, -\dot{\Psi})^T$ and $\underline{v} = (\dot{\xi}, 0, 0)$ be, respectively, the rotational and linear velocity vectors of the spacecraft. Let $\underline{r_0} = (0, -h_0, 0)^T$ be the position of the center of mass of the solidified fuel. Its total linear velocity in the inertial frame is given by

$$\dot{\xi}\underline{u}_\xi + \underline{\omega} \wedge \underline{r} = (\dot{\xi} - \dot{\Psi} h_0)\underline{u}_\xi \ .$$

Therefore, the total kinetic energy of the solidified fuel is

$$T_0 = \frac{1}{2} m_0 (\dot{\xi} - \dot{\Psi} h_0)^2 + \frac{1}{2} I_0 \dot{\Psi}^2 \ .$$

Concerning the N modal masses, since each of them is additionally moving with velocity $\dot{\xi}_i$ with respect to the moving $\dot{\xi}$ tank wall, the total linear velocity is equal to $\dot{\xi} + \dot{\xi}_i + h_i \dot{\Psi}$ for $i = i, \ldots, N$. The kinetic energy of the modal masses is given by

$$T_i = \frac{1}{2} m_i (\dot{\xi} + \dot{\xi}_i + h_i \dot{\Psi})^2 \ , \qquad i = 1, \ldots, N$$

for which the rotary inertial contribution is null as every mass is not considered as an extended body. Analogously, recalling that the masses have a further displacement (than the sole rotation $-\Psi$) from the vertical axis ξ_i, denoting by g the gravity acceleration, the potential energy of the modal masses can be evaluated as

$$U_i = m_i g \left(-h_i (1 - \cos \Psi) - \xi_i \sin \Psi\right) \approx -m_i g \left(h_i \frac{\Psi^2}{2} + \xi_i \Psi\right) \ , \qquad i = 1, \ldots, N \ .$$

Finally, the potential energy due to the springs must be taken into account and it is given by

$$U_i^s = \frac{1}{2} k_i \xi_i^2 \ , \qquad i = 1, \ldots, N \ .$$

Furthermore, the dissipation energy of the each dashpot (due to the sole relative motion of the modal masses with respect to the tank wall) is given by the expression:

$$\mathfrak{I} = \frac{1}{2}\sum_{i=1}^{N} C_i \dot{\xi}_i^2 \ ,$$

in which the coefficients C_i might be written by means of the damping factors of the equivalent dashpot ζ_i and the natural frequencies ω_i as ([33])

$$C_i = 2m_i\omega_i\zeta_i \ , \qquad i = 1, \ldots, N \ .$$

Summing up all the terms, the total kinetic, potential and dissipation energies are found.

More precisely, recalling that $\underline{q} = (\xi, \xi_1, \ldots, \xi_N, \Psi)^T$ and $\underline{Q} = (-F_\xi, 0, M_\eta)^T$, applying Hamilton's principle, the force F_ξ and the momentum M_η can be written as

$$-F_\xi = m_0(\ddot{\xi} - \ddot{\Psi}h_0) + \sum_{i=1}^{N} m_i(\ddot{\xi}_i + \ddot{\xi} + h_n\ddot{\Psi})$$

and

$$M_\eta = I_0\ddot{\Psi} + m_0h_0(\ddot{\xi} - h_0\ddot{\Psi}) - g\sum_{i=1}^{N} m_i\xi_i + \sum_{i=1}^{N} m_ih_i(\ddot{\xi}_i + \ddot{\xi} + h_i\ddot{\Psi}) \ .$$

From the derivation of the Lagrangian function with respect to the ξ_i coordinates, the equation of the i-th mode of sloshing is given by

$$m_i(\ddot{\xi} + \ddot{\xi}_i + h_i\ddot{\Psi}) + k_i\xi_i + C_i\dot{\xi}_i - m_ig\Psi = 0 \ .$$

These equations fully describe the dynamics of the equivalent model for the translational and pitching small oscillatory excitements.

4.2 – Variable mass

The problem of a mechanical system in which the mass varies with time was first investigated at the beginning of the XIX century by the Czech mathematician Graf Georg von Buquoy (see [4, 35]). Attention to this problem was received also by H. Gylden ([17]) when studying the motion of comets and by J.E. Littlewood ([26]) in the context of a two-body problem with a central force of the type $\alpha(t)/r^2$.

The effect of the variation of the mass on the attitude of the body becomes relevant with the appearance of artificial satellites. Indeed, whenever some mass is ejected from a spacecraft, the result is a disturbance torque around the center of mass, which can degrade the control system performance or even cause general

mission failures ([36]). Since the mass expulsion torque is *internally* generated, the fact that it produces a dissipative effect might not be clear on a first analysis. However, when the expelled mass is no longer regarded as part of the spacecraft, the effect of mass expulsion on a spacecraft is to alter the angular momentum, thus dissipating energy. Moreover, the mass expulsion causes the center of mass to shift and the principal axes of inertia to change, thus provoking a dissipation of the rotational energy of the spacecraft.

There are indeed several possible sources of mass expulsion torques. The main types of mass expulsion disturbances (see [3]) are leakage, thrust vector misalignment, impingement of the external plume, venting, anomalous firing time.

Interesting models concerning a mass variable system have been developed in [14, 39, 37]; this problem shows an increasing difficulty as the shape of the spacecraft is more elaborated: from a cylinder-shaped satellite ([14]) to an axisymmetric model ([39]) or a two-body axisymmetric system allowing also for a nozzle ([37]).

Here we review the results presented in [14], which concern the attitude dynamics of a cylinder with variable mass. An explicit solution can be found, although the drawback is that the model does not allow for a nozzle. With reference to [14], we consider a solid right circular cylinder with height equal to $2h$ and basis of radius R. We assume that the cylinder has an initial angular velocity ω_0. Due to combustion, parts of the cylinder become fluid at some instant of time. We denote by C the cylinder shape, while B is the solid part (see Figure 9).

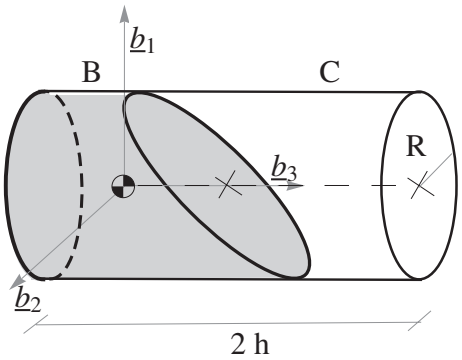

Figure 9 A cylinder shape C of height $2h$ and basis with radius R; the solid part is denoted by B, whose barycenter is at distance d from the right face of the cylinder.

To write the equations of motion, according to [14] we make the following simplifying assumptions:

(i) the motion of the fluid part is axisymmetric with respect to the rigid part and without whirlpools;

(ii) B is axisymmetric at all times so that, denoting by I_1, I_3 the transverse and axial central inertia scalars, we can write the instantaneous central inertia

dyadic as

$$\underline{I} = I_1\ (\underline{b}_1\underline{b}_1 + \underline{b}_2\underline{b}_2) + I_3\ \underline{b}_3\underline{b}_3\ ,$$

where $(\underline{b}_1, \underline{b}_2, \underline{b}_3)$ are a triad of unit vectors fixed in B;

(*iii*) we assume that the velocity of a generic particle relative to C is zero, except at the right end of the cylinder, where, due to the asymmetry, we can assume that $\underline{v} \cdot \underline{n} = u$ with u constant and $\underline{n}$ the outward unit normal to the surface of C.

Denoting by $\underline{M}$ the momentum associated to the external forces with respect to the instantaneous barycenter of the system, say $\underline{M} = M_1\underline{b}_1 + M_2\underline{b}_2 + M_3\underline{b}_3$, the equations describing the attitude dynamics are given by

$$\begin{aligned} M_1 &= I_1\dot{\omega}_1 + (I_3 - I_1)\omega_2\omega_3 + \dot{I}_1\omega_1 - \dot{m}\left(d^2 + \frac{1}{4}R^2\right)\omega_1 \\ M_2 &= I_2\dot{\omega}_2 - (I_3 - I_1)\omega_1\omega_3 + \dot{I}_1\omega_2 - \dot{m}\left(d^2 + \frac{1}{4}R^2\right)\omega_2 \\ M_3 &= I_3\dot{\omega}_3 + \dot{I}_3\omega_3 - \dot{m}\,\frac{R^2}{2}\omega_3\ , \end{aligned} \tag{4.1}$$

where d is the distance of the center of mass from the right face of the cylinder C. The expression for $\dot{I}_1$, $\dot{I}_3$ depends on the way in which the mass distribution is affected by the burning process. If we assume as in [14] that the burning is uniform, then the equations of motion can be explicitly integrated as follows. Since:

$$I_1 = m\left(\frac{1}{4}R^2 + \frac{1}{3}h^2\right)\ , \qquad I_3 = m\frac{R^2}{2}\ ,$$

and since h, R are constant, we obtain:

$$\dot{I}_1 = \dot{m}\left(\frac{1}{4}R^2 + \frac{1}{3}h^2\right)\ , \qquad \dot{I}_3 = \dot{m}\frac{R^2}{2}\ .$$

If the external torque is zero, then (4.1) become:

$$\begin{aligned} \dot{\omega}_1 + \frac{b}{a}\omega_2\omega_3 - \frac{\dot{m}}{m}\frac{c}{a}\omega_1 &= 0 \\ \dot{\omega}_2 - \frac{b}{a}\omega_1\omega_3 - \frac{\dot{m}}{m}\frac{c}{a}\omega_2 &= 0 \\ \dot{\omega}_3 &= 0\ , \end{aligned} \tag{4.2}$$

where

$$a = \frac{1}{4}R^2 + \frac{1}{3}h^2\ , \qquad b = \frac{1}{4}R^2 - \frac{1}{3}h^2\ , \qquad c = \frac{2}{3}h^2\ .$$

The last equation in (4.2) provides $\omega_3(t) = \omega_3(0)$. Introducing the complex angular velocity $\omega_c = \omega_1 + i\,\omega_2$, we get:

$$\frac{\dot{\omega}_c}{\omega_c} = \frac{\dot{m}}{m}\frac{c}{a} + i\,\frac{b}{a}\omega_3(0) \ ,$$

whose solution provides:

$$\frac{\omega_c(t)}{\omega_c(0)} = \left(\frac{m(t)}{m(0)}\right)^{\frac{c}{a}} \ e^{i\,\frac{b}{a}\omega_3(0)\,t} \ .$$

This expression shows that the attitude motion in the transverse direction is of oscillatory type with constant frequency. Assuming that the mass decreases in time, namely that $m(t) < m(0)$ for $t > 0$, and noticing that $c/a > 0$, we conclude that the amplitude of the oscillations decays.

This concludes the discussion of the attitude dynamics of a cylinder with variable mass. We believe that it would be interesting to combine the attitude motion with the orbital motion with variable mass, the so-called Gylden-Meshcherskii problem ([28]), to investigate the coupling between the rotational and orbital dynamics of such complex, though physically interesting, problem.

Acknowledgements

M.C. thanks C. Colombo and F. Bernelli Zazzera for useful suggestions. M.C. was supported by the European Grant MC-ITN Astronet-II. A.C. was partially supported by PRIN-MIUR 2010JJ4KPA_009, GNFM-INdAM and by the European Grant MC-ITN Astronet-II.

REFERENCES

[1] V. I. Arnold: *Proof of a Theorem by A.N. Kolmogorov on the invariance of quasi-periodic motions under small perturbations of the Hamiltonian*, Russ. Math. Surveys, **18** (1963), 13–40.

[2] V. V. Beletskii: *Motion of an Artificial Satellite about its Center of Mass*, Israel program for scientific translations, Jerusalem, 1966.

[3] E. P. Blackburn – R. F. Bohling – F. J. Calloll – D. B. DeBra – B. M. Dobrotin – R. E. Fischell – A. J. Fleig – D. C. Fosth – J. W. Kelly – H. Perkel – R. E. Robertson – J. J. Rodden – A. E. Sabroff – E. D. Scott – C. H. Spenny – B. E. Tinling: *Spacecraft mass expulsion torques*, NASA space vehicle design criteria (guidance and control), NASA SP8034, 1969.

[4] G. von Buquoy: *Weitere Entwickelung und Anwendung des Gesetzes der virtuellen Geschwindigkeiten in mechanischer und statischer Hinsicht*, Leipzig: Breitkopf und Härtel, 1814.

[5] R. Calleja – A. Celletti – R. de la Llave: *A KAM theory for conformally symplectic systems: efficient algorithms and their validation*, J. Differential Equations, n. 5, **255** (2013), 978–1049.
[6] A. Celletti: *Analysis of resonances in the spin-orbit problem in celestial mechanics: The synchronous resonance*, J. Appl. Math. Phys. (Part I), **41**, 174; (Part II) **41** (1990), 453.
[7] A. Celletti: *Construction of librational invariant tori in the spin–orbit problem*, J. of Applied Math. and Physics (ZAMP), **45** (1993), 61–80.
[8] A. Celletti: *Stability and Chaos in Celestial Mechanics*, Springer-Verlag, Berlin; published in association with Praxis Publishing Ltd., Chichester, ISBN: 978-3-540-85145-5, 2010.
[9] A. Celletti – L. Chierchia: *Quasi-Periodic Attractors in Celestial Mechanics*, Arch. Rational Mech. Anal., **191** (2009), 311–345.
[10] G. Colombo – I. I. Shapiro: *The Rotation of the Planet Mercury*, Astroph. J., **145** (1966), 296–307.
[11] A. C. M. Correia – J. Laskar: *Mercury's capture into the 3/2 spin–orbit resonance as a result of its chaotic dynamics*, Nature, **429** (2004), 848–850.
[12] A. H. J. De Ruiter – C. Damaren – J. R. Forbes: *Spacecraft dynamics and control: An introduction*, Chichester: Wiley, 2013.
[13] S. D'Hoedt – A. Lemaitre: *The spin–orbit resonant rotation of Mercury: a two degree of freedom Hamiltonian model*, Cel. Mech. Dyn. Astr., n. 3, **89** (2004), 267–283.
[14] F. O. Eke – S.-M. Wang: *Attitude behavior of a variable mass cylinder*, J. Applied Mech., **62** (1995), 935–940.
[15] P. Goldreich – S. Peale: *Spin–orbit coupling in the solar system*, Astronom. J., n. 6, **71** (1966), 425–438.
[16] J. Guckenheimer – P. Holmes: *Nonlinear Oscillations, Dynamical Systems and Bifurcation of Vector Fields*, Springer-Verlag, 1983.
[17] H. Gylden: *Die Bahnbewegungen in einem Systeme von zwei Körpern in dem Falle, dass die Massen Veränderungen unterworfen sind*, Astron. Nachr., **109** (1884), col. 1–6.
[18] P. C. Hughes: *Spacecraft Attitude Dynamics*, Dover Publications, Toronto, 2004.
[19] A. N. Kolmogorov: *On the conservation of conditionally periodic motions under small perturbation of the Hamiltonian*, Dokl. Akad. Nauk. SSR, **98** (1954), 527–530.
[20] R. Krechetnikov – J. E. Marsden: *Dissipation-induced instabilities in finite dimensions*, Rev. Mod. Phys., **79** (2007), 519–553.
[21] Inarrea M. – V. Lanchares: *Chaotic pitch motion of an asymmetric non-rigid spacecraft with viscous drag in circular orbit*, International Journal of Non-Linear Mechanics, **41** (2006), 86–100.
[22] J. L. Junkins: *Introduction to Dynamics and Control of Flexible Structures*, American Institute of Aeronautics and Astronautics, 1993.
[23] J. Laskar – F. Joutel – P. Robutel: *Stabilization of the Earth's obliquity by the Moon*, Nature, **361** (1993), 615–617.
[24] J. Laskar – P. Robutel: *The chaotic obliquity of the planets*, Nature, **361** (1993), 608–612.
[25] A. Lemaitre – S. D'Hoedt – N. Rambaux: *The 3:2 spin–orbit resonant motion of Mercury*, Cel. Mech. Dyn. Astr., **95** (2006), 213–224.
[26] J. E. Littlewood: *Adiabatic invariance. II. Elliptic motion about a slowly varying center of force*, Ann. Physics, **26** (1964), 131–156.
[27] V. K. Melnikov: *On the stability of the center for time periodic perturbations*, Trans. Moscow Math Soc., **12** (1963), 1–57.

[28] I. V. Meshcherskii: *Works on the Mechanics of Variable-Mass Bodies*, Nauka, Moscow, 1952.
[29] J. Moser: *On invariant curves of area–preserving mappings of an annulus*, Nach. Akad. Wiss. Göttingen, Math. Phys. Kl. II, **1** (1962), 1–20.
[30] S. J. Peale: *The free precession and libration of Mercury*, *Icarus*, **178** (2005), 4–18.
[31] G. Peano: *Sopra lo spostamento del polo sulla terra*, Atti R. Accad. Sci. Torino, **30** (1895), 515–523.
[32] G. Peano: *Sul moto del polo terrestre*, Atti R. Accad. Sci. Torino, **30** (1895), 845–852.
[33] A. I. Raouf: *Liquid Sloshing Dynamics*, Cambridge University Press, Cambridge, 2005.
[34] S. M. Seltzer – J. S. Patel – G. Schweitzer: *Attitude control of a spinning flexible spacecraft*, Computer and Electrical Engineering, **1** (1973), 323–339.
[35] V. Šíma – J. Podolský: *Buquoy's problem*, Eur. J. Phys., **26** (2005), 1037–1045.
[36] S. Soldini – F. Bernelli-Zazzera – M. Vasile: *Attitude Dynamics of ESMO Satellite: Mass Expulsion Torques and Propellant Slosh Model*, Aerotecnica Missili & Spazio, The Journal of Aerospace Science, Technology and Systems, n. 1/2, **92** (2013), 17–26.
[37] J. Sookgaew – F. O. Eke: *Effects of substantial mass loss on the attitude motions of a rocket-type variable mass system*, Nonlinear Dyn. Syst. Theory, n. 1, **4** (2004), 73–88.
[38] V. Volterra: *Sur la thèorie des variations des latitudes*, Acta Math., **22** (1899), 201–358.
[39] S.-M. Wang – F.O. Eke: *Rotational dynamics of axisymmetric variable mass systems*, Trans. ASME, **62** (1995), 970–974.
[40] J. R. Wertz: *Spacecraft Attitude Determination and Control*, Kluwer Academic Publishers, Torrance, CA, 1999.
[41] J. Wisdom: *Rotational dynamics of irregularly shaped natural satellites*, Astron. J., no. 5, **94** (1987), 1350–1360.

Lavoro pervenuto alla redazione il 12 novembre 2014
ed accettato per la pubblicazione il 18 novembre 2014
bozze licenziate il 16 dicembre 2014

Indirizzo degli Autori:
Marta Ceccaroni – Alessandra Celletti – Departments of Mathematics – University of Roma Tor Vergata – Via della Ricerca Scientifica 1 – 00133 – Roma – Italy
E-mail: ceccaron@mat.uniroma2.it – celletti@mat.uniroma2.it